

## A theoretical and chemical view of surface chemistry: Chemisorption and reactions of acetylene

Jérôme Silvestre and Roald Hoffmann

Citation: *J. Vac. Sci. Technol. A* **4**, 1336 (1986); doi: 10.1116/1.573607

View online: <http://dx.doi.org/10.1116/1.573607>

View Table of Contents: <http://avspublications.org/resource/1/JVTAD6/v4/i3>

Published by the AVS: Science & Technology of Materials, Interfaces, and Processing

---

### Related Articles

Flash sample heating for scanning tunneling microscopy: Desorption of 1-octanethiolate self-assembled monolayers in air

*J. Vac. Sci. Technol. B* **31**, 013201 (2013)

New method of calculating adsorption and scattering for Xe-Pt(111) using Direct Simulation Monte Carlo techniques

*J. Vac. Sci. Technol. A* **30**, 061401 (2012)

Gain and loss mechanisms for neutral species in low pressure fluorocarbon plasmas by infrared spectroscopy

*J. Vac. Sci. Technol. A* **30**, 051308 (2012)

Differences in erosion mechanism and selectivity between Ti and TiN in fluorocarbon plasmas for dielectric etch

*J. Vac. Sci. Technol. B* **30**, 041811 (2012)

Investigation of interfacial oxidation control using sacrificial metallic Al and La passivation layers on InGaAs

*J. Vac. Sci. Technol. B* **30**, 04E104 (2012)

---

### Additional information on *J. Vac. Sci. Technol. A*

Journal Homepage: <http://avspublications.org/jvsta>

Journal Information: [http://avspublications.org/jvsta/about/about\\_the\\_journal](http://avspublications.org/jvsta/about/about_the_journal)

Top downloads: [http://avspublications.org/jvsta/top\\_20\\_most\\_downloaded](http://avspublications.org/jvsta/top_20_most_downloaded)

Information for Authors: [http://avspublications.org/jvsta/authors/information\\_for\\_contributors](http://avspublications.org/jvsta/authors/information_for_contributors)

## ADVERTISEMENT



**Aluminum Valves with Conflat® Flanges**

Less Outgassing Than Stainless  
Mate to Stainless Steel Conflats  
Sizes From 2.75 to 14 inch O.D.  
Leak Rate Less Than  $10^{-10}$  SCC/S

Visit us  
at Booth # 300  
in Tampa

Prices & Specifications  
[vacuumresearch.com](http://vacuumresearch.com)



# A theoretical and chemical view of surface chemistry: Chemisorption and reactions of acetylene

Jérôme Silvestre and Roald Hoffmann

Department of Chemistry and Materials Science Center, Cornell University, Ithaca, New York 14853

(Received 22 August 1985; accepted 17 September 1985)

The cluster–surface analogy suggests a similarity between discrete organometallic molecules and surfaces. But the detailed working out of the electronic changes that guide chemisorption and reactivity, here illustrated by acetylene on Pt(111), remains. The translation from delocalized band calculations to a localized chemical picture is made possible by decompositions of the densities of states of an extended surface—adsorbate slab and by the analysis of crystal orbital overlap population curves—scaled bond orders in the solid. The preference of the hydrocarbon for a specific surface site, the strength of its bonding, and its reactivity are determined by a balance of surface—acetylene bonding versus the loss of such bonding within the surface and/or within the organic adsorbate. Surface reconstruction and dissociative chemisorption are merely extremes of this delicate balance.

The combined efforts of organometallic and surface science chemists have taught us that the binding and reactivity of hydrocarbon fragments attached to discrete transition metal clusters and metal surfaces should be similar.<sup>1</sup> An empirical justification for this statement is a simple observation that can be made by inspection of Fig. 1. The latter shows on the left-hand side a number of conceivable adsorption sites for an acetylene on the (111) face of a platinum crystal. Starting from the top, one has C<sub>2</sub>H<sub>2</sub> sitting on a onefold adsorption site, the C–C midpoint falling right above one of the metal atoms. Next, the C–C bond lies parallel to a Pt–Pt bond in what we will call a twofold site. One may want to push the C–C bond into one of the triangles defined by the Pt atoms and a threefold bridging situation is reached. The last straightforward possibility puts the C–C bond across one Pt–Pt bond, thereby defining a twofold perpendicular or fourfold geometry.

On the right-hand side of the figure are depicted four acetylene-containing organometallic molecules, each characterized by x-ray diffraction.<sup>2</sup> From top to bottom, one finds C<sub>2</sub>H<sub>2</sub> bound to a mononuclear *d*<sup>10</sup>-ML<sub>2</sub> unit, a binuclear framework in a parallel geometry, a trinuclear fragment, and a binuclear unit with the M–M bond perpendicular to the C–C axis.

A comparison of each adsorption site of the left with the discrete molecule on its right makes it clear that the *local environment* of the C<sub>2</sub>H<sub>2</sub> is the same in both cases. Assuming an as yet imprecisely geometry-electronic structure relationship, the electronic characteristics of each of the adsorption sites displayed in Fig. 1 should have some similarities with those of the complexes shown at right on the figure. It is our task to delineate and quantify these similarities and the extent to which they do exist. That is what the following discussion is about.

The calculations we carry out in our group are of the extended Hückel type<sup>3(a),3(b)</sup> and makes use of the two-dimensional character of the system via the tight-binding approximation.<sup>3(c)</sup> The surface is simulated by a slab of finite thickness (three layers). The hydrocarbon layer is such that

the coverage is 1/4 so that the experimentally determined<sup>4</sup> (2 × 2) LEED pattern is taken into account.

Let us proceed and bring an acetylene layer on top of the (111) face of platinum in the twofold parallel geometry of 1.

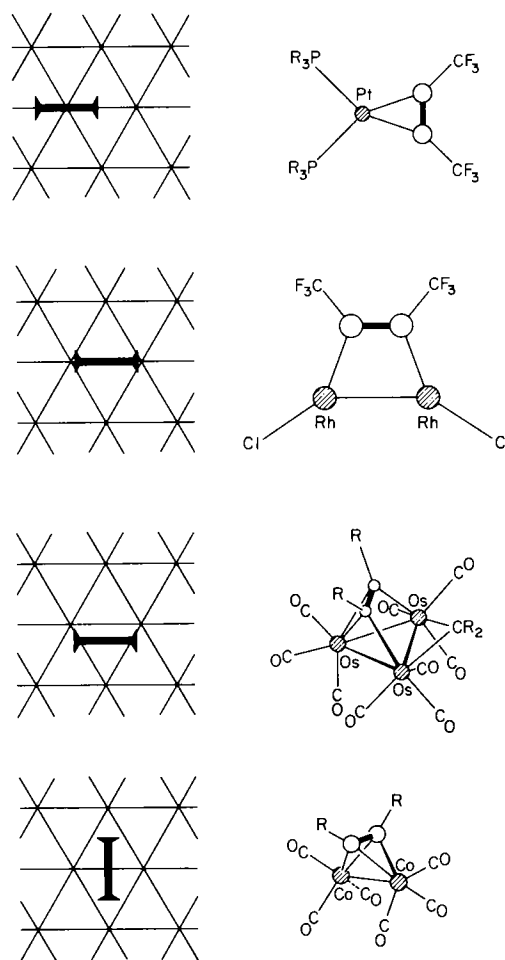


FIG. 1. Left: different adsorption sites for C<sub>2</sub>H<sub>2</sub> on Pt(111). Right: typical mono-, bi-, and trinuclear acetylene complexes in organometallic chemistry.

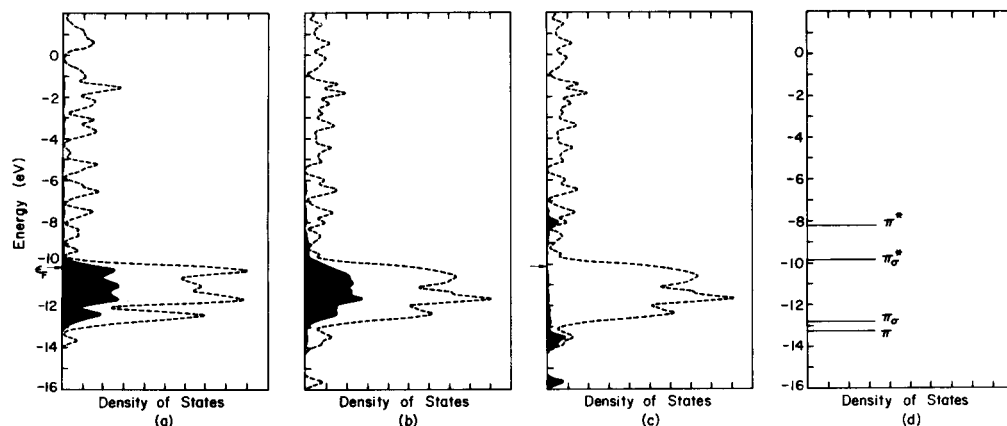
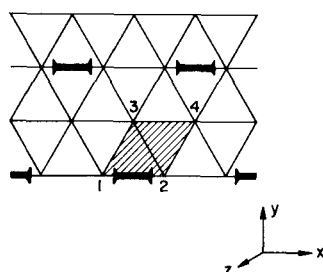


FIG. 2. (a) Contribution of the surface  $d$  states in the slab before interaction. (b) Contribution of the surface  $d$  states in the overall system after interaction. (c) Contribution of the acetylene states in the overall system after interaction. (d) Density of states of the acetylene layer only. The area under each contribution curve is darkened.

The unit cell therefore contains one molecule of acetylene and four Pt atoms in the outermost layer, plus corresponding metal atoms in the lower layers. The left-hand side of Fig. 2 displays the total density of states curve for the bare metal surface. The dark area is a projection of those states which are metal  $d$  in character and belong to the four surface atoms, 1, 2, 3, and 4 of 1. The extreme right plot of the figure



features a pseudo-density of states (DOS) for the acetylene layer only. The peaks evolve as  $\delta$  functions<sup>5</sup> since without the surface the acetylene molecules interact little at this coverage and therefore do not develop any bandwidth.

Putting the acetylenes into contact with the surface alters these two plots as shown in the middle left and right of the figure. Some of the metal  $d$  states initially located just below the Fermi level (arrow) have vanished. Conversely, the dip existing at  $\sim -12.0$  eV in the DOS of the slab-only has been filled and more states are now present in this energy region. Interestingly enough this shift of states is observed by Plum-

mer and co-workers using angle-resolved photoelectron spectroscopy.<sup>6</sup>

Turning to the acetylene levels, interaction with the surface has spread them considerably. The black area of the middle right plot defines the states centered on  $C_2H_2$  in the composite system. Gone is the clear cut splitting between  $\pi$ ,  $\pi_\sigma$ ,  $\pi_\sigma^*$ , and  $\pi^*$ . The surface dilutes all these states.

What is the fate of each of the  $C_2H_2$  levels? Figure 3 answers this question. From left to right is plotted the contribution to the total DOS separately of  $\pi$ ,  $\pi_\sigma$ ,  $\pi_\sigma^*$ , and  $\pi^*$ . The curves have been magnified by a constant ratio for better viewing and the total DOS curves are omitted in the pictures. However, the integration curves are left in. Those count up the number of states under consideration on sweeping up across the energy scale. The stick marks position the corresponding states in the absence of  $C_2H_2$ /surface interaction. The following observations can be made: The bonding  $\pi$  orbital does not interact much; it is slightly pushed down in energy by a few tenths of an eV. The other bonding MO is more involved and experiences a lot of interaction; 70% of the states are depressed in energy by more than 3 eV. Also at the Fermi level roughly 20% of them are empty; some forward donation from  $C_2H_2$  to the surface has occurred.

It is however, in the behavior of  $\pi_\sigma^*$  that we find the most drastic electronic effects of the chemisorption. Initially all empty, more than 50% of the states are now filled. The contact of  $C_2H_2$  with the surface has spread the  $\pi_\sigma^*$  band broadly. Starting at  $-9.8$  eV as a single peak, this band has now a width of  $\sim 7$  eV, ranging from  $-13.5$  to  $-6.5$  eV! A tre-

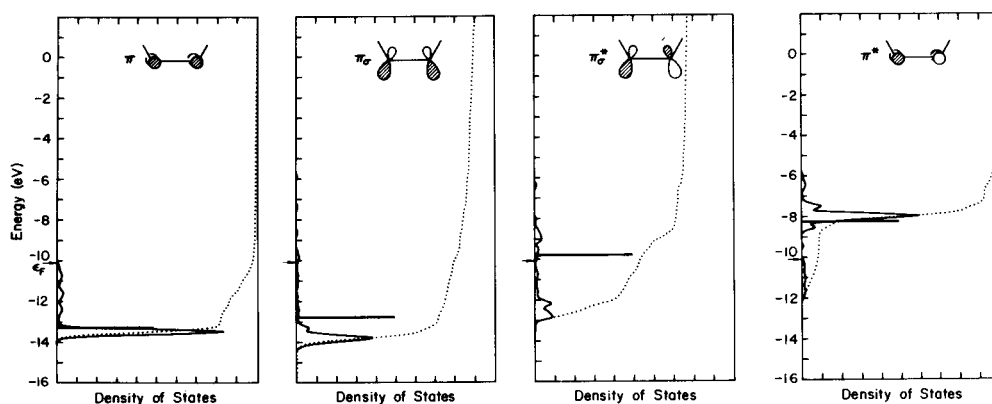
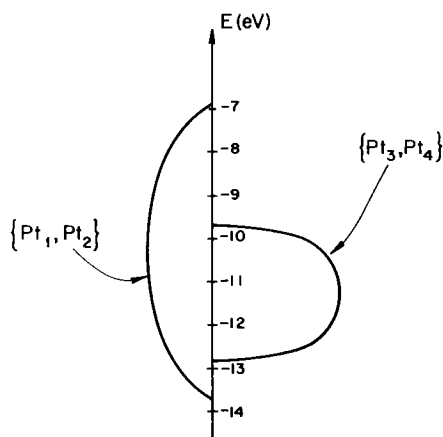


FIG. 3. From left to right: contributions of  $\pi$ ,  $\pi_\sigma$ ,  $\pi_\sigma^*$ , and  $\pi^*$  to the DOS of  $C_2H_2$  in the twofold geometry. The curves are magnified by a factor of 10.

mendous amount of back donation takes place here and  $\pi_{\sigma}^*$ , empty to begin with, winds up occupied by 1.06 electrons.

Finally  $\pi^*$  is moderately destabilized, by 0.5 eV. The extent of  $\pi^*$  contribution in the overall picture appears to be small but, still, 8% of the states fall below  $\epsilon_F$  and thus  $\pi^*$  is occupied with 0.160 electrons. We will see eventually how a geometrical perturbation forces  $\pi^*$  to get more involved in the action going on at the acetylene/surface contact.

Now we must unearth the levels of the surface which drive the chemisorption. One can use a similar approach to that described above and decompose the DOS curve into projections corresponding to orbitals with different angular momentum, before and after chemisorption. Before we illustrate this process for the  $\sigma$  type of interaction, one needs to "check" which surface atoms of the set {1,2,3,4} (see 1) are mostly involved in binding the acetylene. From a simple topological standpoint, it is clear that Pt<sub>1</sub> and Pt<sub>2</sub> feel C<sub>2</sub>H<sub>2</sub> more than Pt<sub>3</sub> and Pt<sub>4</sub>. In 2 are shown schematic projected



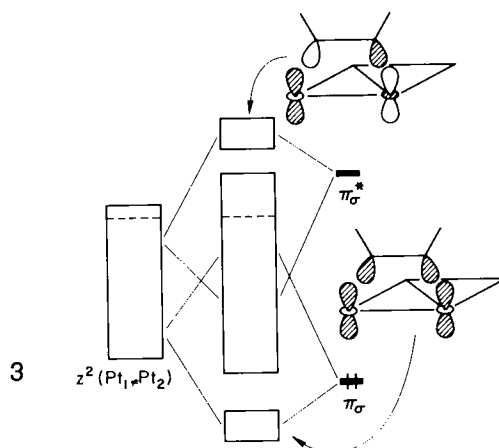
2

DOS curves for the two subsets of Pt atoms belonging to the unit cell within the outermost layer of the slab. Before interaction with C<sub>2</sub>H<sub>2</sub>, all these  $d$  states are contained within the window  $-9.5/-13.0$  eV.

Now the  $d$  states centered on Pt<sub>1</sub> and Pt<sub>2</sub> are spread over  $\sim 7$  eV, whereas those descending from Pt<sub>3</sub> and Pt<sub>4</sub> remain packed in their initial range. Consequently the metal  $d$  states

that interact most with C<sub>2</sub>H<sub>2</sub>, as anticipated, are centered on Pt<sub>1</sub> and Pt<sub>2</sub>.

Figure 4 shows at left the projection of the  $\pi_{\sigma}$  states, in the middle that of the  $z^2$  states on Pt<sub>1</sub> and Pt<sub>2</sub>, and at the right the projection of  $\pi_{\sigma}^*$  states. One can see that the peak of the bottom of the  $z^2$  band matches perfectly the peak of  $\pi_{\sigma}$  at  $-13.8$  eV. Similarly the  $z^2$  band has a nice feature at  $-9.0$  eV which finds some counterpart in the  $\pi_{\sigma}^*$  curve. The change of slope in the integration line of  $\pi_{\sigma}^*$  reflects an accumulation of states around  $-9.0$  eV. Finally, between  $-12.0$  and  $-13.0$  eV, one finds peaks common to  $\pi_{\sigma}^*$  and  $z^2$ . What we have in hand here is an interaction between the whole  $z^2$  band of {Pt<sub>1</sub>, Pt<sub>2</sub>} and both  $\pi_{\sigma}$  and  $\pi_{\sigma}^*$ . We may depict this in the more conventional frame of an interaction diagram as in 3. The dashed line refers to the Fermi level.



3

Note that in the main block there should be a few states carrying  $\pi_{\sigma}^*$  character below states involving  $\pi_{\sigma}$ . Also from this picture it is clear that the  $z^2$  band is depleted of some of its electron density upon coordination of C<sub>2</sub>H<sub>2</sub>. Both Pt<sub>1</sub> and Pt<sub>2</sub> actually see their electron density in  $z^2$  reduced by 0.282 electrons each.

Representative interactions may be drawn out as shown in 3. The two combinations are certainly analogous to those holding an acetylene in a binuclear organometallic complex.<sup>2(b)</sup>

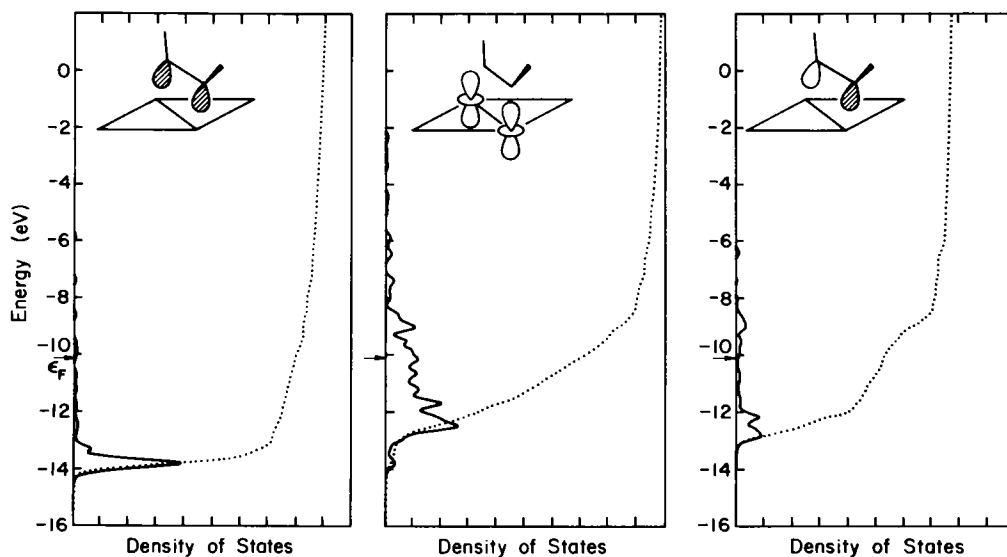


FIG. 4. From left to right: contributions of  $\pi_{\sigma}$ ,  $z^2$  (Pt<sub>1</sub>, Pt<sub>2</sub>), and  $\pi_{\sigma}^*$  to the DOS of the C<sub>2</sub>H<sub>2</sub>/Pt(111) system of the twofold geometry. The curves are magnified by a factor of 10.

What is the fate of those electrons which are destabilized by the antibonding component of the  $z^2$ - $\pi_\sigma$  interaction? They move mostly into the bulk. Around the Fermi level there are many levels involving interactions between surface atoms and the inner layer ones. These states act as an empty "reservoir" and take up to the overflow of electrons generated by the  $z^2$ - $\pi_\sigma$  interaction. Neighboring metal atoms in the outermost layer and not engaged in bonding with the adsorbate act in a similar fashion. On the average, an inner layer atom is computed to gain 0.150 electrons in the process of chemisorption in this geometry. In other words, electrons are transferred from filled states of the surface to empty states in the bulk via the intermediacy of  $\pi_\sigma$ . The interaction at work here was encountered and discussed in previous studies.<sup>7</sup>

The way the  $\pi$  system of  $C_2H_2$  mixes with the surface  $d$  states may be analyzed along the same lines. Notice that in Fig. 3 we can easily locate (i) the bonding combination between bonding metal  $d$  states and the bonding MO of  $C_2H_2$ , and (ii) the antibonding states between antibonding metal orbitals and antibonding MO's of  $C_2H_2$ . These two types of states in the composite system fall outside the bulk of the surface  $d$  band as depicted in 3 and are primarily centered on  $C_2H_2$ . The reason for this is that the center of gravity of the  $d$  band falls inevitably between the donor ( $\pi$ ,  $\pi_\sigma$ ) and the acceptor ( $\pi^*$ ,  $\pi_\sigma^*$ ) levels of the adsorbate. A useful way to see the states drowned in the metal  $d$  band makes use of the crystal orbital overlap population, or COOP,<sup>8</sup> curves. These are overlap population weighted densities of states. What is plotted here is the contribution (positive or negative) of a group of levels at a certain energy makes to bonding in a specified bond of the system. An application and example of such curves is provided in Fig. 5. At the left and on the same graph are the overlap population curves for the C-C bond (solid line) and the  $Pt_{1,2}$ -C bond (dotted line). On the right is the corresponding curve for the  $Pt_1$ - $Pt_2$  bond. Let us sweep through the energy scale and enumerate the interactions we encounter along the way. Everything on the right (left) of the vertical axis is bonding (antibonding) between the two atoms under consideration.

At  $-13.9$  eV one finds  $\pi_\sigma + [z^2(1) + z^2(2)]$ . These states are bonding (+) within the acetylene, bonding between  $Pt_1$  and  $Pt_2$ , and bonding between  $C_2H_2$  and the substrate. At  $-13.5$  eV are states of the type  $\pi + [y-z(1) + yz(2)]$ . It is amusing to notice that the maxima in the dotted (Pt-C) and solid (C-C) lines of Fig. 5(a) do not

coincide. The C-C curve peaks at  $-13.6$  eV, whereas the Pt-C one peaks at  $-13.9$  eV. Each curve has its maximum where the other features a shoulder. This comes from the fact that maximum C-C bonding is provided by  $\pi$  rather than  $\pi_\sigma$  and maximum Pt-C bonding results from the  $\sigma$  interaction rather than the  $\pi$  one. Between  $-13.0$  and  $-12.0$  eV are states bonding between the metal and  $C_2H_2$  and involving  $\pi_\sigma^*$ :  $\pi_\sigma^* + [z^2(1) - z^2(2)]$ .<sup>9</sup> All the features appearing in these COOP curves may be analyzed<sup>10</sup> using this pseudolocalized type of interaction but what needs to be emphasized most is that many states antibonding between the metal atoms and empty before chemisorption wind up well below the Fermi level after contact with the acetylene and therefore become populated. The result is that *the bonding within the surface is weakened*, as attested to by the drop of overlap population between  $Pt_1$  and  $Pt_2$ , from 0.136 to 0.077.

We have so far discussed and analyzed in some detail the chemisorption of  $C_2H_2$  in a twofold parallel geometry on the Pt(111) surface. Next we discuss the overall trends that come out of computations for the alternative sites described in Fig. 1. Our working basis is Table I. First, the threefold bridging geometry is clearly the most stable and favorable. This agrees with a number of experimental<sup>4</sup> and theoretical<sup>11</sup> results. Looking at the overlap population entry, one sees that in the sequence onefold, twofold, threefold, and fourfold, the acetylene triple bond is more and more weakened.<sup>12</sup> This holds also for the metal-metal bonding within the exposed layer. Summing all the Pt-C overlap populations at each geometry, the surface- $C_2H_2$  bonding varies in the reverse order. A large number is obtained for more bridging geometries. We return to these opposite effects shortly.

A glance at the occupation numbers gives a hint as to why the fourfold geometry is so strongly bound. In this geometry both the electron loss from  $C_2H_2$  ( $\pi$  and  $\pi_\sigma$  depopulated) and gain ( $\pi^*$  and  $\pi_\sigma^*$  populated) are the largest of all sites. Also it is easy to check that, overall,  $C_2H_2$  gains electron density in each geometry—slightly more than half of an electron on the average. This leads us to the next entry in Table I, the charges of the surface atoms. These are initially negatively charged (10.125 electrons). From the numerical results, it is apparent that the more a surface atom is in contact with  $C_2H_2$ , the larger is its electron density loss.

A final remark deals with the fact that the amount of charge lost by the surface atoms is larger than that gained by  $C_2H_2$ . As mentioned earlier, the difference goes into the

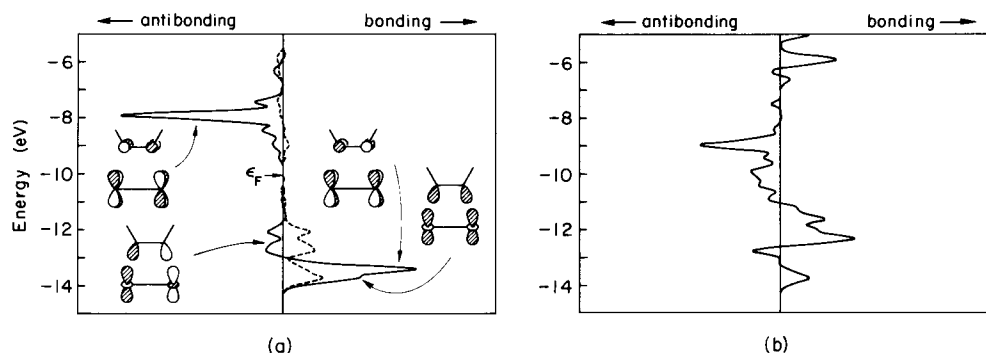


FIG. 5. (a) COOP curve for the C-C (solid line) and Pt-C (dotted line) bonds. (b) COOP curve for the  $Pt_1$ - $Pt_2$  bond. Both plots refer to the  $C_2H_2$ /Pt(111) system in the twofold geometry.

TABLE I. Bonding characteristics of several acetylene absorption sites.

$C_2H_2$	Bare surface				
Binding energy <sup>a</sup> (eV)		-3.56	-4.68	-4.74	-4.46
Fermi level	-10.02	-10.00	-10.09	-10.07	-9.97
Overlap population					
C-C	1.703	1.405	1.319	1.206	1.080
Pt <sub>1</sub> -Pt <sub>2</sub>	0.136	0.126	0.077	0.088	-0.024
Pt <sub>2</sub> -Pt <sub>3</sub>	0.136	0.139	0.126	0.067	0.062
Pt <sub>1</sub> -Pt <sub>4</sub>	0.136	0.130	0.126	0.149	0.062
Pt <sub>1</sub> -C <sup>b</sup>		0.295	0.543	0.517	0.330
Pt <sub>3</sub> -C		0.001	0.005	0.193	0.266
Occupations					
$\pi^*$	0.0	0.078	0.166	0.330	0.533
$\pi_\sigma^*$	0.0	0.811	1.059	1.028	0.893
$\pi_\sigma$	2.0	0.733	1.588	1.591	1.566
$\pi$	2.0	1.959	1.956	1.731	1.530
Net charges					
Pt <sub>1</sub>	+0.125	-1.111	-0.600	-0.535	-1.115
Pt <sub>2</sub>	+0.125	-0.084	-0.600	-0.535	-1.115
Pt <sub>3</sub>	+0.125	-0.035	-0.125	-0.690	-0.435
Pt <sub>4</sub>	+0.125	-0.035	-0.125	-0.125	-0.435

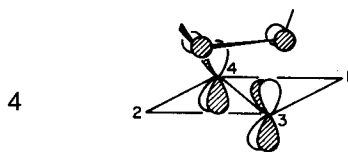
<sup>a</sup> Taken as the difference:  $E(\text{geometry}) - E(\text{slab}) - E(C_2H_2)$  in eV. The negative signs mean  $C_2H_2$  is always bound.

<sup>b</sup> The carbon atom here is the closest to the particular Pt atom under consideration.

bulk.

The overall picture that emerges from these calculations is that of a compromise that must be reached for a strong, yet not dissociative chemisorption; the bonding within both the adsorbate and the substrate must be weakened.

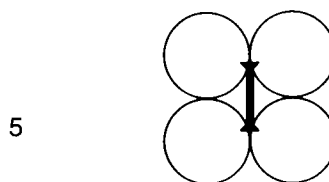
Two extreme situations can doom any possibility of attaining this compromise. The first case results from an excessive weakening of the metal-metal bonding within the surface. This is illustrated by the fourfold bridging geometry. The Pt<sub>1</sub>-Pt<sub>2</sub> overlap population is *negative* or to put it another way, the Pt-Pt bond is gone—destroyed. We would like to think of this situation as one that leads to surface reconstruction. For the particular case<sup>13</sup> of  $C_2H_2$  on Pt(111), this will not happen since the acetylene will bind without damage in the threefold site. Still, can we single out a specific interaction that leads to the disruption of bonding



between Pt<sub>1</sub> and Pt<sub>2</sub>? The answer is yes, and is illustrated in 4 from a top view. The  $\pi$  orbital of  $C_2H_2$  matches locally the symmetry of the top (initially empty) of the  $yz$  band; a tremendous electron transfer takes place here in a series of

states overwhelmingly Pt-Pt antibonding.

Alternatively, it is the carbon-carbon bond that may be ruined upon chemisorption. To illustrate this case we turn to the chemisorption of  $C_2H_2$  on the (100) face of iron. Previous cluster calculations<sup>14</sup> by Anderson point to a fourfold adsorption site such as in 5. Figure 6 presents the projection



of the acetylene states after chemisorption. This is to be compared with Fig. 2. Again the initial levels of  $C_2H_2$  are indicated with stick marks and the Fermi level with an arrow. The latter sits in the vicinity of the  $-8.0$  eV mark, about 2 eV higher than in the Pt case. Obviously the more electropositive character of Fe compared to Pt is the source of this difference.

It is apparent that  $\pi$  and  $\pi_\sigma$  are pushed down upon interaction. Not by much though; for instance, the  $\pi$  states are depressed in energy less than in the twofold Pt(111) case. Recalling that the strength of the interaction is governed by the energy difference between combining orbitals, the fact that the  $d$  block of Fe is moved up by  $\sim 2$  eV with respect to that of Pt, i.e., further away from  $\pi$  (and  $\pi_\sigma$ ) makes it clear

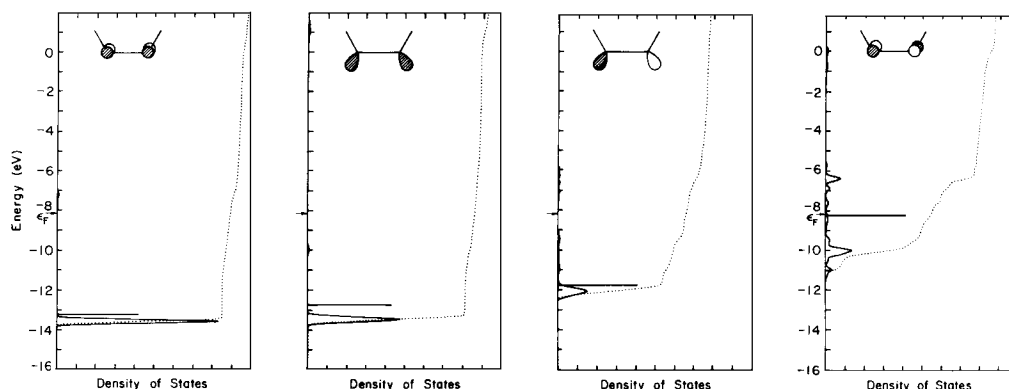
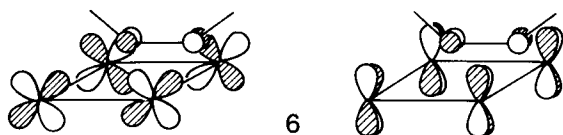


FIG. 6. From left to right: contributions of  $\pi$ ,  $\pi_\sigma$ ,  $\pi_\sigma^*$ , and  $\pi^*$  to the DOS of  $C_2H_2$  for the  $C_2H_2/Fe(100)$  system. The curves are magnified by a factor of 4.2.

why the  $C_2H_2$  bonding orbitals are stabilized less by the Fe(100) surface than by Pt(111).

By the same argument, one anticipates stronger interactions involving  $\pi_\sigma^*$  and  $\pi^*$  in the Fe case. A glance at the right-hand side plots of Fig. 5 shows that this is indeed true. Please focus on the integration curve: at  $\epsilon_F$ ,  $\pi_\sigma^*$  is occupied by 1.35 electrons and  $\pi^*$  is filled with 1.065 electrons. These numbers are much larger than any of the corresponding ones encountered in Table I dealing with the  $C_2H_2/Pt(111)$  system. The weakening of the acetylenic triple bond results from a tremendous back-donation from the metal into C–C antibonding orbitals. This is particularly true for  $\pi^*$  of  $C_2H_2$ . The interactions at work here are combinations of the type in 6. The C–C overlap population initially of 1.703 drops dra-



matically to 0.965. The ultimate outcome of this finding is that *no barrier is computed to breaking  $C_2H_2$  into two CH fragments on this surface*. The chemisorption would be predicted to be dissociative and is found<sup>15</sup> experimentally to occur at  $\sim 100$  K. Certainly this implies not much of a barrier.

In conclusion, using a deconvolution technique for the density of states of an adsorbate/substrate system, we are able to single out localized states involved in anchoring an acetylene to a metal surface. Both the geometrical choice made by the hydrocarbon and its reactivity are controlled by the system's ability to reach a compromise; the price of the gain in binding energy must be evenly distributed over the loss of bonding within the adsorbate and the surface. Surface reconstruction and dissociative chemisorption are merely extreme alternatives.

## ACKNOWLEDGMENTS

Our work was generously supported by the Office of Naval Research. It also owes much to the favorable atmosphere for surface science created at Cornell by the Materials Science Center funded by the National Science Foundation.

- <sup>1</sup>(a) N. D. S. Canning and R. J. Madix, *J. Phys. Chem.* **88**, 2437 (1984); (b) E. L. Muettterties and J. Stein, *Chem. Rev.* **79**, 479 (1979); (c) E. L. Muettterties, *Chem. Soc. Rev.* **11**, 283 (1982); (d) E. L. Muettterties, T. N. Rhodin, E. Rand, C. F. Brucker, and W. R. Pretzer, *Chem. Rev.* **79**, 91 (1979); (e) N. Sheppard, *J. Mol. Struct.* **80**, 163 (1982).
- <sup>2</sup>(a) For  $ML_n$ , see: S. Otsuka and A. Nakamura, *Adv. Organomet. Chem.* **14**, 245 (1970); (b) For  $M_2L_{2n}$ , see: D. M. Hoffman, R. Hoffmann, and C. R. Fisel, *J. Am. Chem. Soc.* **104**, 3858 (1982), and references therein. (c) For  $M_3L_{3n}$ , see: E. Sappa, A. Tiripicchio, and P. Braunstein, *Chem. Rev.* **83**, 203 (1983).
- <sup>3</sup>(a) R. Hoffmann, *J. Chem. Phys.* **39**, 1397 (1963); (b) R. Hoffmann and W. N. Lipscomb, *ibid.* **36**, 2176 (1962); (c) For the implementation of the E.H. formalism to generate band structures, see: M.-H. Whangbo, R. Hoffmann, and R. B. Woodward, *Proc. R. Soc. London A* **366**, 231 (1979).
- <sup>4</sup>R. J. Koestner, M. A. Van Hove, and G. A. Somorjai, *Chem. Tech.* **13**, 376 (1983); *J. Phys. Chem.* **87**, 209 (1983); G. A. Somorjai, *Chem. Soc. Rev.* **13**, 321 (1984).
- <sup>5</sup>The two  $\pi$  degeneracies are lifted upon bending of the hydrogens away from the surface [see Ref. 2(b)].
- <sup>6</sup>M. R. Albert, L. G. Sneddon, W. Eberhardt, F. Greuter, T. Gustafsson, and E. W. Plummer, *Surf. Sci.* **120**, 19 (1982).
- <sup>7</sup>J.-Y. Saillard and R. Hoffmann, *J. Am. Chem. Soc.* **106**, 2006 (1984).
- <sup>8</sup>T. Hughbanks and R. Hoffmann, *J. Am. Chem. Soc.* **105**, 1150 (1983).
- <sup>9</sup>The convention here is to take + (–) as bonding (antibonding). In the –12.0/–13.0 eV region the  $z^2/z^2$  interaction is antibonding but just above –13.0 all the other atomic contributions on Pt<sub>1</sub> and Pt<sub>2</sub> are bonding, hence the negative and then abruptly positive COOP at the right in Fig. 5 in this energy window.
- <sup>10</sup>J. Silvestre and R. Hoffmann, *Langmuir* (in press).
- <sup>11</sup>See for example, S. P. Mehandru and A. B. Anderson, *Appl. Surf. Sci.* **19**, 116 (1984).
- <sup>12</sup>The C–C bond distance is kept constant throughout; the overlap population is therefore a scaled bond order.
- <sup>13</sup>Sheppard and co-workers have noticed that a small change in the metal-metal distance could explain the fourfold adsorption site on Ni(111); B. J. Bandy, M. A. Chesters, M. E. Pemble, G. S. McDougall, and N. Sheppard, *Surf. Sci.* **139**, 87 (1984).
- <sup>14</sup>A. B. Anderson and S. P. Mehandru, *Surf. Sci.* **136**, 398 (1984).
- <sup>15</sup>T. N. Rhodin, C. F. Brucker, and A. B. Anderson, *J. Phys. Chem.* **82**, 894 (1978).